DOI: 10.1002/chem.200800283

Heterolytic Cleavage of Peroxide by a Diferrous Compound Generates Metal-Based Intermediates Identical to Those Observed with Reactions Utilizing Oxygen-Atom-Donor Molecules

Gerard T. Rowe,[a] Elena V. Rybak-Akimova,[b] and John P. Caradonna*[a]

Abstract: Under cryogenic stopped-flow conditions, addition of 2-methyl-1-phenylprop-2-yl hydroperoxide (MPPH) to the diiron(II) compound, $[Fe_2(H_2Hbamb)_2(NMeIm)_2]$ (**1**; NMeIm = *N*-methylimidazole; H_4HBamb: 2,3-bis(2-hydroxybenzamido)dimethylbutane) results in heterolytic peroxide O–O bond cleavage, forming a high-valent species, **2**. The UV/Vis spectrum of **2** and its kinetic behavior suggest parallel reactivity to that seen in the reaction of **1** with oxygen-atom-donor (OAD) molecules, which has been reported previously. Like the interaction with OAD molecules, the reaction of **1** with MPPH proceeds through a three step process, assigned to oxygen-atom transfer to the iron center to form a high-valent intermediate (**2**), ligand rearrangement of the metal complex, and, finally, decay to a diferric μ-oxo compound. Careful examination of the order of the reaction with MPPH reveals saturation behavior. This, coupled with the anomalous non-Arrhenius behavior of the first step of the reaction, indicates that there is a preequilibrium peroxide binding step prior to O–O bond cleavage. At higher temperatures, the addition of the base, proton sponge, results in a marked decrease in the rate of O–O bond cleavage to form **2**; this is assigned as a peroxide deprotonation effect, indicating that the presence of protons is an important factor in the heterolytic cleavage of peroxide. This phenomenon has been observed in other iron-containing enzymes, the catalytic cycles of which include peroxide O–O bond cleavage.

Keywords: bioinorganic chemistry · iron · methane monooxygenase · peroxides · stopped-flow methods

Introduction

The activation of dioxygen in diverse, iron-dependent oxygenase systems such as cytochrome P450, phenylalanine hydroxylase, and soluble methane monooxygenase (sMMO) is generally understood to proceed through the two-electron reduction of dioxygen to form either an end-on η^1 iron (hydro/alkyl) peroxide species or a side-on η^2 iron peroxide species.[1–3] The resulting heterolytic cleavage of the iron-peroxo O–O bond in the presence of H^+ yields one equivalent of H_2O/ROH and a high-valent iron-oxo intermediate, the electrophilic oxygen atom of which is ultimately inserted into a substrate C–H bond. Current efforts are directed at modeling this process by using synthetic analogue systems to better understand the mechanism by which 1) dioxygen activation and 2) peroxide O–O bond cleavage occurs.[4–7] One particularly challenging aspect of modeling the function of these enzymatic systems is effecting the heterolytic cleavage of the peroxide O–O bond to form an Fe^{IV}=O species that will then oxidize substrates with significant C–H bond strengths. Many iron-based monooxygenase model systems are reported to promote homolytic cleavage of peroxide O–O bonds, resulting in the production of hydroxyl or alkoxyl radical species.[6,8] We report herein a detailed low-temperature kinetic characterization of the metal-based intermediates observed after the heterolytic cleavage of the O–O bond of 2-methyl-1-phenylprop-2-yl hydroperoxide (MPPH) by the diferrous complex, $[Fe_2(H_2Hbamb)_2(NMeIm)_2]$ (**1**; NMeIm = *N*-methylimidazole; H_4HBamb: 2,3-bis(2-hydroxybenzamido)dimethylbutane Figure 1), a synthetic analogue system that was previously shown to catalyze the oxidation of alkanes to alcohols.[4]

Early evidence suggesting the ability of small molecule iron compounds to utilize peroxides in a non-hydroxyl radi-

[a] G. T. Rowe, Prof. J. P. Caradonna
Department of Chemistry, Boston University
Boston, MA 02215 (USA)
Fax: (+1) 617-353-6466
E-mail: caradonn@bu.edu

[b] Prof. E. V. Rybak-Akimova
Department of Chemistry, Tufts University
Medford, MA 02115 (USA)

Supporting information for this article is available on the WWW under http://dx.doi.org/10.1002/chem.200800283.

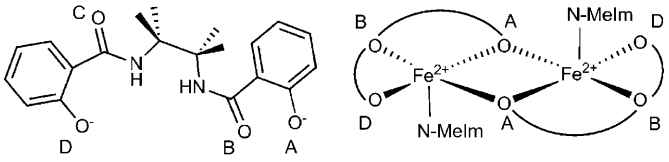

Figure 1. Structure of the ligand and assembled metal complex, **1**. NMeIm = *N*-methylimidazole.

cal dependent fashion to oxidize substrates was provided by Groves and co-workers, in which a ferrous perchlorate/perchloric acid system in anhydrous acetonitrile was shown to catalyze the stereoselective hydroxylation of cyclohexanol to *cis*-cyclohexane-1,2-diol as the major product.[9] Subsequent studies by Sawyer et al. concluded that this anhydrous system ($<0.005\%$ H_2O) was also capable of oxidizing phosphines and sulfides, and causing dehydrogenation of cyclohexadiene in the absence of perchloric acid.[10] In each case, an Fe^{IV}=O species was proposed as the active oxidant due to the observed reactivity behavior that is uncharacteristic of radical species. However, the presence of modest (2%) concentrations of H_2O led to the activation of chemistry consistent with the formation of the hydroxyl radical. Interpretation of this chemistry is further challenged by the realization that Fe^{IV}=O species can arise from either heterolytic or homolytic peroxide O–O cleavage pathways involving Fe^{II} or Fe^{III}, respectively.[8]

Differentiating iron-based homolytic versus heterolytic peroxide cleavage pathways by the examination of product distributions remains difficult, as oxygen-based radicals are themselves potent oxidants and can lead to similar products.[6,11,12] In this report, we utilize the mechanistic probe peroxide MPPH to define the mode of iron-induced peroxide O–O cleavage.[11] As seen in Scheme 1, homolytic cleavage of the O–O peroxide bond of MPPH results in a radical species that undergoes very rapid ($2.2\times10^8\ s^{-1}$) β-scission rearrangement to produce one equivalent each of acetone and benzyl radical. The less-potent benzyl radical will then react further to produce a known series of products that can be detected by GC, GC/MS or LC/MS analytical methods.[4,11] Heterolytic cleavage of the O–O bond results in the formation of the corresponding alcohol, 2-methyl-1-phenylprop-2-ol (MPP-OL) concomitant with the expected formal transfer of an oxygen atom to the metal center. The utilization of MPPH in place of *tert*-butyl hydroperoxide or hydrogen peroxide has proven useful in establishing the participation of freely diffusing oxygen-based radical species in systems previously believed to oxidize substrates solely by means of a metal-based oxidant.[6]

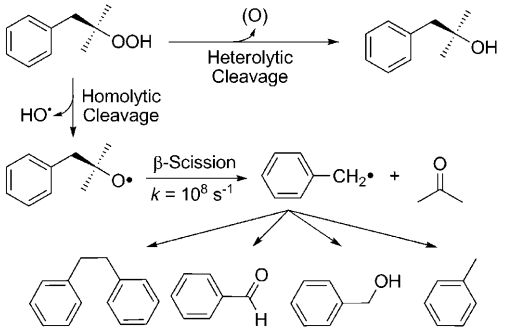

Scheme 1. Heterolytic/homolytic decomposition pathways of MPPH.

We have previously reported that **1** is capable of utilizing MPPH as the oxygen atom source to hydroxylate alkanes such as cyclohexane ($BDE_{C-H}=414\ kJ\,mol^{-1}$; BDE = bond disassociation energy) in excess of 200 turnovers with >98% O-atom mass balance, yielding the major product cyclohexanol (>200 turnovers) with a small amount of cyclohexanone (5 turnovers) resulting from the oxidation of cyclohexanol; MPP-OL was the sole peroxide cleavage product indicating that only Fe-catalyzed heterolytic O–O bond cleavage occurred.[4] A series of reports show that other selected metal systems also induce heterolytic cleavage of the O–O bond of MPPH. The titanosilicate epoxidation catalyst, TS-1, is capable of utilizing MPPH in the epoxidation of alkenes in greater efficiency than hydrogen peroxide or *t*-butyl hydroperoxide.[13] Heme model systems were also observed to promote heterolytic cleavage of MPPH.[5] Interestingly, the heme systems were reported to produce varying amounts of homolytic products as well, and the extent to which this occurred decreased with the presence of more electron withdrawing heme substituents. Because the heterolytic pathway has been implicated in mechanistic studies of our system, and in light its demonstrated oxidative catalytic abilities,[4] we believe that **1** proceeds through an Fe^{IV}=O intermediate species in its reaction with oxygen-atom-donor (OAD) molecules and peroxides. Starting with a **1**-peroxo adduct, O–O bond heterolysis would result in the formal two-electron oxidation of the metal compound, concomitant with oxygen transfer, with the formation of an Fe^{IV}=O species as the most likely mechanism. This is supported by the compound's subsequent reaction chemistry that has been revealed in previous low-temperature stopped-flow studies with OAD molecules.[14] In this current work, we study the mechanism by which binuclear [Fe^{II},Fe^{II}], **1**, reacts with MPPH to form a high-valent iron intermediate through the use of low-temperature stopped-flow UV/Vis spectroscopy.

Results and Discussion

Reaction of 1 with MPPH and comparison to OAD: The reaction of a 100-fold excess (pseudo-first order) of MPPH with **1** at 188 K in a 70:30 (v/v) mixture of dichloromethane/dimethylformamide exhibits triphasic behavior as observed by stopped-flow UV/Vis spectroscopy. The reaction proceeds through three observed steps: i) the fast ($k=10(1)\ M^{-1}\,s^{-1}$) pseudo-first order growth of an intermediate species, **2**, with a chromophore centered around $\lambda=435$ nm, followed by ii) the slower ($k=0.05\ s^{-1}$) conversion to a second intermediate species, **3**, with a chromophore with $\lambda_{max}=$

438 nm ($\varepsilon = 4000\ cm^{-1}\,M^{-1}$), and iii) the decay to a final species, **4**, at a slow rate ($k = 0.005(1)\ s^{-1}$ at 190 K) with $\lambda_{max} =$ 445 nm ($\varepsilon = 7500\ cm^{-1}\,M^{-1}$). In previous stopped-flow studies of the reaction of **1** with OAD molecules, the same triphasic behavior was seen (Table 1),[14] and in the reaction with MPPH, the three successive reaction steps are similarly assigned as i) oxygen atom transfer to one of the Fe^{2+} centers of **1** to form **2**, assigned as an Fe^{IV}=O species, ii) ligand rearrangement to **3**, in which bridging phenolate groups from the ligands shift to a terminal position, and iii) collapse of the Fe^{IV}=O moiety onto the neighboring ferrous iron center to form the inert, diferric μ-oxo (Fe^{III}-μ-O-Fe^{III}) **4**. The stoichiometry of the reaction is shown in Equations (1–3).

$$\mathbf{1} + \text{MPPH} \xrightarrow{k_1} \mathbf{2} + \text{MPP-ol} \quad (1)$$

$$\mathbf{2} \xrightarrow{k_2} \mathbf{3} \quad (2)$$

$$\mathbf{3} \xrightarrow{k_3} \mathbf{4} \quad (3)$$

The rate laws used to fit the kinetic data are shown in Equations (4–6).

$$-\frac{d[\mathbf{1}]}{dt} = \frac{d[\mathbf{2}]}{dt} = k_{obs}[\mathbf{1}] = k_1[\mathbf{1}][\text{MPPH}] \quad (4)$$

$$-\frac{d[\mathbf{2}]}{dt} = \frac{d[\mathbf{3}]}{dt} = k_2[\mathbf{2}] \quad (5)$$

$$-\frac{d[\mathbf{3}]}{dt} = \frac{d[\mathbf{4}]}{dt} = k_3[\mathbf{3}] \quad (6)$$

As seen in Figure 2, the reaction of **1** with MPPH results in the formation of species with identical chromophores as with an OAD molecule, leading us to propose the analogous mechanism shown in Scheme 2. In addition, in the reaction of **1** with MPPH, only heterolytic cleavage products have been observed, implying the same 2-electron chemistry occurs in both MPPH and OAD (i.e., homolytic O–O bond cleavage would imply one-electron chemistry, resulting in a different iron-oxygen species).

Assignment of steps and factors affecting kinetic parameters: The initial k_1 reaction of MPPH with [Fe^{II},Fe^{II}], **1**, exhibits first-order dependence for both peroxide and **1** concentrations, while subsequent kinetic steps (k_2 and k_3) are oxidant independent. The k_1 reaction does, however, exhibit saturation behavior; the plot of initial rate versus MPPH concentration deviates from linearity at high MPPH concentrations, and appears to posses an asymptotic shape

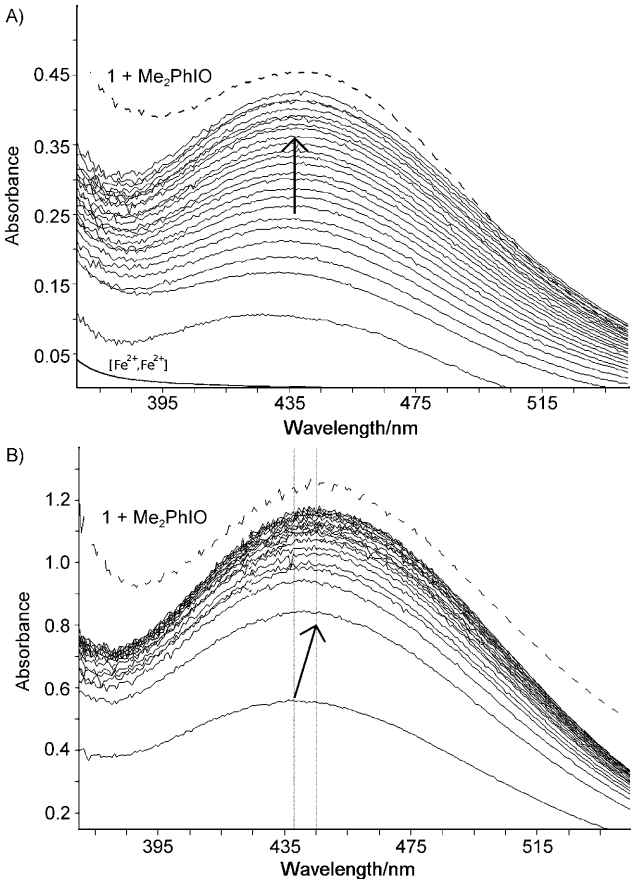

Figure 2. Diode array stopped-flow UV/Vis spectra showing the reaction of **1** with MPPH (——) at 198 K; A) after 3.5 s forming a species with $\lambda_{max} = 438$ nm and B) after 380 s, shifting to $\lambda_{max} = 445$ nm. Superimposed onto both spectra is the analogous spectrum of the species resulting from the reaction of **1** with the OAD, 2,6-dimethyliodosylbenzene in equivalent time regimes (-----).

(Figure 3). This saturation behavior would be expected for a rapid, preequilibrium binding process resulting in a reactive species that converts to **2**. This assignment is supported by the anomalous non-Arrhenius behavior observed at low temperatures in studies of **1**+MPPH versus **1**+MPPH+ proton sponge (1,8-bis(dimethylamino)-naphthalene) (see below).

Following the formation of **2**, the absorbance at $\lambda =$ 438 nm continues to increase at a slower rate than the initial formation of **2**. This second step is assigned as a ligand rearrangement of **2** to form **3**. This rate of this second process is independent of oxidant concentration, and is similarly unaffected by the presence of base. In addition, studies of **1** with one-electron oxidants have shown that following rapid, oxidant-dependent oxidation (comproportionation with oxidized diferric **1**, $k = 4.3(5) \times 10^2\ M^{-1}\,s^{-1}$; 1,1′-trimethylene-2,2′-dipyridinium diiodide, $k =$

Table 1. Kinetic and activation parameters at 188 K.

Oxidant	$\Delta H^{\ddagger}$ [kJ mol^{-1}]	$\Delta S^{\ddagger}$ [J mol^{-1} K]	$\Delta G^{\ddagger}_{188\,K}$ [kJ mol^{-1}]	k_1 [M^{-1} s^{-1}]	k_2 [s^{-1}]	k_3 [s^{-1}]	ref.
MPPH	30(4)	−60(18)	41(7)	10(1)	0.05(2)	0.005(1)[a]	[b]
MPPH + 1.3 equiv proton sponge	–	–	–	9(1)	0.08(2)	–	[b]
p-CN-DMANO	36(4)	21(12)	33(6)	$4.7(2) \times 10^3$	0.3(1)	0.003(1)	[14]
Me_2PhIO	–	–	–	69(5)	0.3(1)	–	[14]

[a] Rate measured at 193 K. [b] This work.

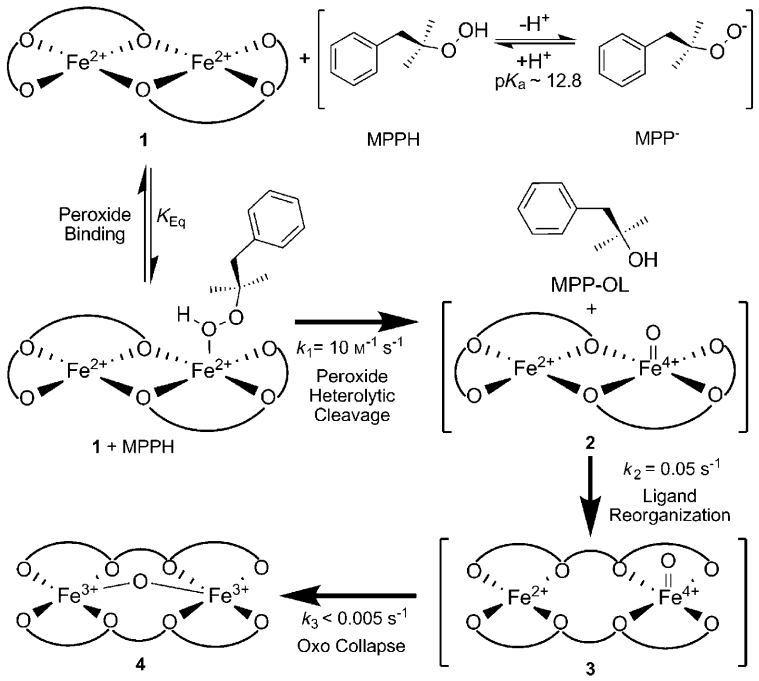

Scheme 2. Proposed reaction scheme. Rates reported at 188 K.

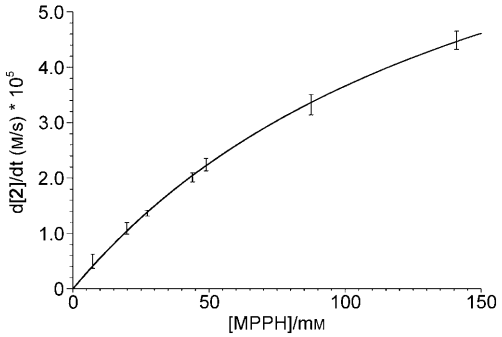

Figure 3. Plot of initial rate versus MPPH concentration exhibiting saturation behavior. Curve fit to Michaelis-Menten equation. Each data point represents the average of at least 5 runs. [**1**] = 0.2 mM. Rates measured at 188 K.

$2.4(6)\times10^{2}\,M^{-1}\,s^{-1}$; $[TBA]_3[Mo(CN)_8]$, $k = 5.2(5)\times10^{4}\,M^{-1}\,s^{-1}$; at 188 K) of the diferrous core of **1**, the resulting mixed-valence compound continues to exhibit an increase in the absorbance of its chromophore ($\lambda = 436$ nm) at a significantly slower rate independent of oxidant, and is assigned as a ligand reorganization resulting in species **3** (Scheme 2).[14]

Direct experimental evidence supporting such an oxidation-state driven ligand reorganization arises from X-ray crystallographic studies on a series of related ligand systems in which the nature of the linker group (-$(CH_2)_n$-, $n = 2$–5) between the diamide moieties was altered.[15] Comparative structural studies of three sets of [Fe^{II},Fe^{II}] and [$Fe^{III}(\mu$-$OMe)_2Fe^{III}$] complexes show conversion of the μ-η^2-$O_{phenolate}$–μ-η^1-$O_{carbonyl}$ binding motif in the diferrous compounds (and by inference in **2**) to the terminal $O_{phenolate}$–$O_{carbonyl}$ in the diferric compounds (and by inference **3** and **4**).[15] This "phenolate/amide carbonyl" (PAC) shift is reminiscent and perhaps chemically/electronically analogous to the μ-(η^2,η^1)- to terminal "carboxylate" shift observed to occur upon oxidation of the reduced forms of the active site diferrous cores in soluble methane monooxygenase and class II ribonucleotide reductase.[16–19] Such a shift is proposed to open coordination sites on the metal centers for dioxygen binding thereby generating a more flexible binuclear core that can undergo rearrangements to accommodate the structural constraints imposed by the one- and two-electron reductions of dioxygen and subsequent O–O bond cleavage to generate the proposed [Fe^{IV},Fe^{IV}=O]⇄[Fe^{III},Fe^{V}=O] or [$Fe^{IV}(\mu$-$O)_2Fe^{IV}$] reactive species.[16,20] Computational simulations led to the hypothesis that the μ-(η^2,η^1)-carboxylate bridge breaks between the first and second-electron reduction of dioxygen (i.e., with formation of the bound peroxo species), concomitant with formation of a hydrogen-bonding interaction with an iron-bound water ligand. Interestingly, low-temperature stopped-flow spectroscopic studies suggest that the PAC-shift for the synthetic complexes occurs after the initial one-electron (chemical) or two-electron (reaction of diferrous core with OAD molecules[14] or heterolytic cleavage of MPPH) process. Similarly, both the enzymatic carboxylate shift and the synthetic model PAC shift are readily reversible upon reduction of the ferric centers, suggesting a thermodynamic preference for the bridging structures in the fully reduced binuclear cores and the presence of relatively small activation energies for both the forward and reverse processes indicating a closeness in absolute energy between the limiting structures.[21] It currently remains unclear in the absence of detailed spectroscopic and computational studies what electronic (and hence chemical) role the coupling of the two metal centers has on the energy profile of the initial intermediate formation process (intermediate **2**) before the PAC-shift and how the energy content (and hence reactivity properties) of the intermediate (species **3**) is altered as a consequence of this rearrangement.

The final step in the reaction with MPPH results in the slow formation of the inert diferric μ-oxo compound **4**, which has been independently synthesized and previously characterized.[14] **4** is incapable of oxidizing substrate in the presence of MPPH; homolytic O–O bond cleavage occurs instead.[4] In addition, irradiation of **4** with short-wave UV light ($\lambda \approx 250$ nm) in the presence of cyclohexane and air re-

sults in no observable formation of cyclohexanol or cyclohexanone. These data indicate that the μ-oxo[Fe^{III},Fe^{III}] complex is inert and does not readily convert either thermally or photochemically into a species that supports catalytic C–H bond oxidation in the presence of MPPH.

The observed MPPH-based kinetic behavior is consistent with data we reported earlier for the reaction of **1** and OAD molecules, in which an oxidant-dependent process was followed by two oxidant-independent steps that ultimately result in the formation of an inert diferric μ-oxo compound (**4**). However, unlike its reaction with OAD molecules, the initial k_1 reaction of **1** with MPPH is remarkably slower at low temperatures, with the peroxide exhibiting rates that are 7 and 470 times slower than those seen in the reactions with the OAD molecules 2,6-dimethyliodosylbenzene (Me_2PhIO) and 4-(dimethyl-amino)benzonitrile N-oxide (*p*-CN-DMANO), respectively (Table 1). Based on the sensitivity of k_1 to the nature of the oxidant used, this step was previously assigned as an X–O bond-breaking reaction that results in the production of a high-valent iron intermediate and deoxygenated OAD molecule/alcohol.[14] If this assignment is correct, the data indicate that either the peroxide O–O bond strength is discernibly stronger than the I–O[22] or the N–O[23] bonds (both with $BDE_{X-O} \approx 260\ kJ\,mol^{-1}$) of the OAD molecules previously utilized, or alternatively, the transition state is simply higher in energy because heterolytic cleavage of the peroxide O–O bond results in the initial formation of a charged alkoxide species in an organic solvent system, or some combination of both possibilities.

In light of the current findings, however, this explanation cannot be entirely true. The data show a lack of correlation between the rate constants k_1 with the X–O bond enthalpies (as seen from the effectively equivalent bond enthalpies for the PhIO and amine N-oxide). This discrepancy is understandable from the analysis of the activation parameters, where the k_1 values do not increase with a lowering of the activation enthalpy as one would expect for an elementary bond breaking reaction (Table 1). Instead, the k_1 values exhibit a strong dependence on the entropy of activation, which would be expected for a two-step reaction with a rapid (but left-lying) preequilibrium binding step. In such a case, both the oxidant binding and inner-sphere O-atom transfer processes would contribute to the overall observed rate constant k_1, and the activations parameters are composite values.

Effect of proton sponge on the reaction: To better understand if the binding affinity of MPPH to the iron center was a factor in the rate of the k_1 reaction, 1.1 equivalents of proton sponge ($pK_a = 12.1$; in water at 25 °C) were combined with the solution of MPPH ($pK_a \approx 12.8$; in water at 20 °C)[24] used in the stopped-flow experiment with the intent to deprotonate the hydroperoxide ([proton sponge] = 27 mM, [MPPH] = 25 mM). If the rate of the reaction of MPPH with **1** is sensitive to the fraction of peroxide that is bound to the ferrous iron complex, then increasing the Lewis basicity of the entering MPPH moiety by removal of a proton is expected to increase the value of k_1. Alternatively, if the proton sponge is insufficiently basic to deprotonate the hydroperoxide at such low temperatures, it should be capable of deprotonating the hydroperoxide once it is bound to the metal center at which point the hydroperoxide acidity is expected to increase.

Although the addition of proton sponge has no discernible effect on the k_1 rate at 188 K ($10\ M^{-1}\,s^{-1}$ for MPPH versus $9\ M^{-1}\,s^{-1}$ for MPPH/proton sponge), its presence has a much more dramatic effect at temperatures greater than 208 K ($528\ M^{-1}\,s^{-1}$ for MPPH versus $375\ M^{-1}\,s^{-1}$ for MPPH/proton sponge at 228 K) as seen in Figure 4. At these higher

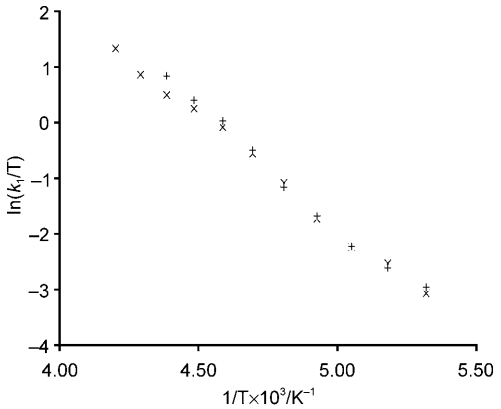

Figure 4. Eyring plot of the k_1 process in the reaction of **1** with MPPH from 188 K to 228 K (+) and MPPH in the presence of proton sponge from 188 K to 238 K (×). Data points are an average of at least 3 runs.

temperatures, proton sponge causes a marked slowing of the reaction with respect to MPPH. We attribute this divergence to the presence of a deprotonated MPPH-**1** complex. Because a deprotonation effect causes a decrease in the k_1 rate, the decrease in rate cannot be attributed to peroxide binding, as deprotonation of the metal-bound hydroperoxide is expected to increase the binding affinity to the metal center. Instead, the differences are attributed to the role that protonation plays in the cleavage of the O–O bond and the stability of the resulting alcohol/alkoxide. The rate difference may reflect the relatively higher pK_a values of alcohols with respect to their corresponding peroxides. In the proton-deficient environment found in the CH_2Cl_2/DMF solvent system, heterolytic cleavage of the peroxide O–O bond would result in an anionic alkoxide, which is expected to be a higher energy situation than generation of the corresponding neutral alcohol.

The differences in k_1 values observed for MPPH and MPPH/proton sponge at higher temperatures may result from a general base effect on the catalyst itself rather than the effects of peroxide deprotonation, but this possibility is ruled out based on the results of a previous experiment in which exogenous base (*p*-cyanodimethylaniline) was added to the stopped-flow mixture.[14] In these experiments, the addition of up to a 10-fold excess of base with respect to iron complex had no effect on the k_1 rate; the k_2 and k_3 rates

were similarly unaffected. Consequently, we attribute the observed differences in the k_1 rate of the reactions of **1** with MPPH and MPPH/proton sponge as arising from the differential rates of O–O bond cleavage of the protonated and deprotonated forms of the peroxide bound to the ferrous iron center, respectively.

Non-Arrhenius and saturation behavior: Close inspection of the Eyring analysis of the k_1 reaction of **1** with MPPH reveals what appears to be a non-linear temperature dependence of $\ln(k/T)$ (see Figure 4 and Figure S5 in the Supporting Information). Non-Arrhenius behavior has been observed in other systems, and has several possible causes.[25] In our system, the most likely origin of the deviation from linearity is the initial k_1 reaction being a composite of a pre-equilibrium peroxide-binding step followed by an O–O bond cleavage step. A shift of the binding equilibrium constant with temperature can cause the apparent activation energy to change, and manifest as non-linearity in the Eyring plot.

This assignment is supported by the observation of saturation kinetic behavior in MPPH concentration (Figure 3). A fit to the Michaelis–Menten equation by using non-linear least-least squares methods gives an apparent K_m value of approximately 160 mM, indicating that MPPH binds weakly to **1**. Saturation behavior is not frequently observed in non-enzymatic systems, but examples exist in the literature,[26] and this behavior should be observable, in principle, for any system in which a rapid pre-equilibrium binding step exists.

Potential biological relevance: The equivalent nature, as determined by low temperature stopped-flow spectroscopic studies, of the reaction of diferrous **1** with OAD molecules[14] and the mechanistic probe peroxide MPPH that has undergone heterolytic O–O bond cleavage indicates the formation of an equivalent reactive intermediate (**2**) that then follows an oxidant independent progression through rearranged species **3** before collapsing to the catalytically inert μ-oxo diferric complex, **4**. Although the thermodynamic activation parameters for the formation of **2**, assigned as an [Fe^{II}, Fe^{IV}=O] core, are expectedly different for the OAD and MPPH reactions, the k_2 and k_3 steps representing a ligand reorganization and collapse of the reactive species to the mutual end product, respectively, are equal. These data reflect the generation of an identical binuclear species that than follows a common chemical channel. Such behavior is entirely expected based on previous studies demonstrating the ability of **1** to catalyze the oxidation of cyclohexane ($BDE_{C-H}=414\,kJ\,mol^{-1}$) to cyclohexanol utilizing PhIO (TON = 57, 47% efficiency)[27] or MPPH (TON = 230, 98% efficiency)[4] as the oxidant. We therefore propose that **1** represents a credible functional analogue of the reduced active site binuclear center of sMMO based on i) the ability of **1** to catalyze the catalytic oxidation of alkanes to alcohols,[4,27] ii) data showing that **1** induces heterolytic cleavage of the alkyl peroxide MPPH,[4] iii) observed parallel chemistry reported previously[14] and herein describing the chemical consequences and reaction progression of reacting OAD molecules and MPPH with the reduced diferrous core of **1** (1:1 stoichiometry), iv) the equivalence of the electronic spectra generated by the reaction of **1** and MPPH or a number of different OAD molecules, and v) the striking similarity of the electronic spectra of **3** and the kinetically competent intermediate of sMMO (kinetic **Q**).[14] Although **3** [Fe^{II}, Fe^{IV}=O] is formally two electron equivalents reduced from the diferryl core of kinetic and spectroscopic **Q**, the above noted properties suggest that the detailed investigation of the reactivity and spectroscopic properties of **3** is relevant to understanding binuclear iron monooxygenase chemistry and that a critical review of the structural assignment of the kinetic **Q** species of sMMO as a [Fe^{IV}(μ-O)$_2$$Fe^{IV}$] moiety (spectroscopic **Q**) is warranted.[14]

An elegant comparative study assessing the abilities of spectroscopically characterized binuclear [LFe^{IV}(μ-O)$_2$$Fe^{IV}$L] and mononuclear [L($CH_3CN$)$Fe^{IV}$=O] complexes containing the same ligand L to perform H-atom abstraction with 9,10-dihydro-anthracene ($BDE_{C-H}=310\,kJ\,mol^{-1}$) as substrate showed that the mononuclear Fe^{IV}=O complex reacts 100 times more rapidly in the substoichiometric H-atom abstraction reaction (42% yield; 0.42 turnover) than the [Fe^{IV}(μ-O)$_2$$Fe^{IV}$] complex (≈100% yield, 1 turnover), independent of the fact that the high-valent binuclear complex has a higher oxidation/reduction potential than the mononuclear Fe^{IV}=O species ($E_{1/2}=760$ mV versus Fc/Fc^+ and 490–670 mV, respectively).[28] The observed lower reactivity of synthetic mononuclear Fe^{IV}=O complexes reported to date versus the kinetic **Q** of sMMO are thought to arise from the fact that the model systems examined have all been low spin iron(IV) complexes, where DFT calculations support the assertion that high spin iron(IV) centers, such as those found in sMMO, have enhanced reactivity versus low spin iron(IV) complexes with respect to H-atom abstraction (and C–H oxidation) processes.[29,30] The substoichiometric ability of a thermally stable low-spin mononuclear Fe^{IV}=O complex to oxidize the C–H bond of cyclohexane (29% yield; cyclohexanol, 0.03 equiv produced; cyclohexanone, 0.13 equiv produced)[31] supports this assertion. These data, in part, were used to support a proposal in which the highly reactive active site oxidant in sMMO is unmasked only when substrate is present in the active site and that the [Fe^{IV}(μ-O)$_2$$Fe^{IV}$] intermediate effectively serves as a repository for the oxidizing equivalents that are made available by isomerization of the less reactive "diamond core" species to an intermediate with a terminal oxo group such as an [Fe^{III},Fe^{V}=O] species.

The experimental and mechanistic implications of this conversion proposal are intriguing and significant. Immediately evident would be the real possibility that the nature/structure of the reactive intermediate assigned as **Q** in sMMO would be different in the absence and presence of substrate. To date, no such ambiguities have been noted, although as discussed earlier,[14] no unambiguous evidence has been presented showing that the kinetic **Q** is the same species as the spectroscopic **Q**. Similarly, detailed stopped-flow

kinetic studies have concluded that the kinetic **Q** is catalytically competent towards substrate oxidations. The possibility may exist that the opening of the $[Fe^{IV}(\mu\text{-}O)_2Fe^{IV}]$ core is significantly slower than the subsequent substrate oxidation step such that kinetic evidence for an $[Fe^{III},Fe^{V}{=}O]$ species would be absent. Indeed, kinetic studies involving the oxidation of nitrobenzene by **Q** show no difference nor lag between the rates of **Q** decay and nitrophenol formation.[32] While the stopped-flow spectroscopic evidence is consistent with the interpretation that either the kinetic **Q** represents the active hydroxylating species or that it is in equilibrium with the active hydroxylating species, the presence of such an interconversion would require a reevaluation of temperature-dependent kinetic data for substrate oxidations, as such processes would no longer be treated as single step reactions but as composite process involving at least two distinct steps. It is also interesting to speculate about the nature of the triggering mechanism for the substrate-dependent "diamond" core opening process as sMMO is a promiscuous enzyme capable of oxidizing a wide range of substrates from methane to linear and branched alkanes, to polyaromatics and cage substrates.

An alternative mechanism has been proposed by us[4,14,27] and others[2,33,34] in which the active species is a terminal oxidant that is generated directly during the decomposition of the peroxide adduct. We have earlier suggested the possibility that the $[Fe^{IV}(\mu\text{-}O)_2Fe^{IV}]$ core may reside along an autodecay pathway of the reactive species **Q** to the resting state diferric active site.[14] The absence of experimental evidence demonstrating the equivalence of the kinetic and spectroscopic **Q** species (by showing the ability of the spectroscopic **Q**, $[Fe^{IV}(\mu\text{-}O)_2Fe^{IV}]$, to oxidize substrates of challenging C–H bond strengths) coupled with the observed collapse of species **3** to **4** are consistent with assignment of the $[Fe^{IV}(\mu\text{-}O)_2Fe^{IV}]$ core as residing on an active site salvage pathway. In addition, the close similarity between kinetically competent **3** ($\lambda_{max}=438$ nm, 30% DMF/CH_2Cl_2) and the kinetic **Q** species ($\lambda_{max}\approx420$ nm) argues against the latter containing an $Fe^{V}{=}O$ moiety, as electronic spectra of $Fe^{IV}{=}O$ and $Fe^{V}{=}O$ groups are expected to be different. The 1:1 stoichiometry of **1**:MPPH experimentally measured to be necessary for the generation of **2** and **3** is inconsistent with the formation of a $[Fe^{IV}(\mu\text{-}O)_2Fe^{IV}]$ core for **3**. Thus, while the chemistry observed for **1** may reflect an entirely different manifold of chemistry than what occurs in the sMMO system, our mechanistic data support the ability of a terminal $Fe^{IV}{=}O$ moiety to mimic not only the electronic spectrum assigned as the kinetically competent **Q** species, but also many aspects of its ability to catalytically oxidize alkanes to alcohols. Furthermore, these data raise the possibility that the observed $[Fe^{IV}(\mu\text{-}O)_2Fe^{IV}]$ core may not reside on the catalytic cycle but on an autodecay pathway not relevant to product formation.[14]

Although the mechanistic and spectroscopic characterizations of models systems will refine our knowledge of chemical constraints that play a role in understanding binuclear iron metalloenzymes, these data reflect transformations and processes that occur in small molecules, devoid of the protein matrix. Nonetheless, these model systems[4,14,27,28] help define and highlight potential pathways and focus interest on experiments designed to unambiguously differentiate between the various chemically realistic possibilities in biochemical/biophysical studies on the natural enzyme systems.

The decrease in the reaction rate of **1** with MPPH in the presence of proton sponge is consistent with the defined role that protons play in the active sites of oxygen activating enzymes. If the trend of divergent rates between the reaction of MPPH with **1** in the presence and absence of proton sponge continues to room temperature (298 K), the difference in rate between the two would become quite significant, with the protonated MPPH reacting much faster than the deprotonated form. If the presence or absence of a proton can have such a large effect on the rate or mode of peroxide cleavage, nature would optimize the availability of protons to stabilize key transition states in oxygenase catalytic cycles, such as those between compounds **P** of sMMO or P450 and their respective high-valent intermediate species. Both enzymes utilize dioxygen by first reducing it to peroxide and then inducing cleavage of the O–O bond, resulting in the formal transfer of an oxygen atom to the iron center and the eventual release of water with the addition of two protons. In kinetic studies of sMMO with dioxygen, the rates of both formation and decay of **P** exhibited a sharp decrease with increasing pH. Indeed, in the presence of buffer with pH > 8.5, the compound **P** of sMMO would not form at all, even though the decay of the oxygen bound compound **O** is pH independent.[35] It was concluded, based on these pH dependence data, that the processes forming both **P** and **Q** are accompanied by the delivery of one proton each, ultimately resulting in heterolytic O–O bond cleavage and concomitant release of water.

Theoretical models of the conversion of **P** to **Q** in sMMO do not include protonation events of the bound peroxide,[20,36,37] and typically afford homolytic cleavage of the peroxide O–O bond to generate the diferryl, di-μ-oxo compound that has been spectroscopically identified as **Q**.[38] Based on our studies, it may be possible that a diferryl, terminal-oxo species forms first from the heterolytic cleavage of a hydroperoxide O–O bond, and then, in the absence of substrate, collapses to a diferryl, di-μ-oxo species as a less reactive decay product. The chromophore of the kinetically competent **Q** as determined by stopped-flow UV/Vis spectroscopic studies exhibits a chromophore around $\lambda=420$–430 nm,[39,40] which is quite similar to the chromophore of **3** ($\lambda=438$ nm), which is assigned as a ferryl terminal-oxo compound.

The results of our study of **1** with MPPH are also consistent with a kinetics investigation of the formation of compound I in human erythrocyte catalase in the presence of various organic peroxide and peracid alternative substrates. If the pH of the buffer solution is raised sufficiently to deprotonate the substrate, the rate of compound I formation sharply decreased.[41] In the formation of compound I, heterolytic cleavage of the deprotonated peroxy or peracid O–O bond would result in the formation of an anionic spe-

cies, which would benefit from the presence of a readily available proton counterion. The possibility does exist, however, that the approach of a charged species into the catalase active site is impeded, resulting in the observed decrease in rate of compound I formation. The reason for this observed phenomenon has not been unambiguously determined. Based on the above model and enzymatic data, the availability and timing of proton addition to the bound iron-peroxide species during its cleavage plays an important factor in lowering the energy of the heterolytic cleavage pathway.

Conclusion

We have shown that the iron-based intermediate formed from the heterolytic cleavage of the O–O bond of the probe peroxide MPPH by **1** is identical to that formed from the reaction with OAD, though the reaction proceeds at a much slower rate with the peroxide. As a result of this, it is possible to observe saturation behavior of the formation of **2** at high MPPH concentrations, and this behavior is attributed to the k_1 reaction being a composite of a peroxide binding preequilibrium step followed by heterolytic O–O bond cleavage. This assignment of a composite reaction step is corroborated by the non-Arrhenius behavior of the reaction observed at low temperatures.

Addition of proton sponge to the reaction mixture decreases the rate of O–O bond cleavage, but only at higher temperatures; there is no observable effect of proton sponge on the k_1 rate at 188 K. This is assigned as a peroxide deprotonation effect, and is informed by similar effects observed in enzymatic systems in which peroxide O–O bond cleavage is slowed or stopped in sufficiently alkaline conditions.

Experimental Section

Materials and methods: Compound **1**[27] and MPPH[4,42] were synthesized according to previously published procedures. The peroxide content of MPPH was determined to be >98% by iodometric titration.[43] Metal ion impurities were excluded from all glassware involved in peroxide synthesis and handling by soaking in a solution of aqueous EDTA (50 mM) for at least 12 h prior to use. Glassware with ground glass joints was strictly avoided throughout the synthesis and handling of MPPH. 2-Methyl-1-phenylprop-2-yl alcohol (98%) was obtained from Sigma–Aldrich. Proton Sponge (1,8-bis-(dimethylamino)naphthalene) was obtained from Aldrich and used without further purification. Prior to use, dimethylformamide (Pharmco, HPLC grade) was processed through a PureSolv solvent purification system from Innovative Technologies. Unstabilized dichloromethane was obtained from Fisher and was distilled over calcium hydride before use. All solvents used in air-sensitive work were thoroughly degassed by subjecting them to at least six successive freeze-pump-thaw cycles, after which they were transferred to an inert atmosphere glove box, in which all solution preparations were carried out.

WARNING! MPPH is an organic peroxide. *The original synthetic procedure calls for distillation of the extracted peroxide/ether solution, but this resulted in an explosion in our lab*. Gentle removal of solvent by blowing a stream of N_2 is recommended as a substitute.

2-Methyl-1-phenylprop-2-yl hydroperoxide (MPPH): 2-Methyl-1-phenylprop-2-yl alcohol (15.8 g, 0.11 mol) was added to a flat-bottomed boiling flask equipped with a cross-shaped stirrer bar. A mixture of 70% hydrogen peroxide (25 mL, 0.66 mol) and sulfuric acid (1.5 mL) was added by addition funnel to the rapidly stirring alcohol over the course of 10 min. Once the addition was complete, the reaction vessel was immersed in an oil bath maintained at 43 °C and stirred rapidly for 12 h. Water (150 mL) was then added to the mixture and the resulting solution was extracted twice with pentane (75 mL). The pentane washings were washed with water and dried by stirring with magnesium sulfate (3 g) for 20 min. The mixture was then filtered and the solvent removed by blowing a stream of dry N_2 over the surface until an oil remained. The oil was solidified by addition of a seed of previously crystallized MPPH and placement in a −40 °C, which afforded crystalline solid within 20 min. Prior to use, MPPH was recrystallized from pentane (30 °C) until iodometric titration confirmed >98% activity. Isolated yield: 5 g, 30%. ^{1}H NMR ($CDCl_3$): δ = 1.209 (s, 6.0), 2.883 (s, 2.0), 7.222 (m, 3.0), 7.288 (m, 2.3), 7.379 ppm (s, 1.0); ^{13}C NMR: δ = 24.1, 44.7, 83.4, 126.6, 128.3, 130.8, 137.9 ppm.

Stopped-flow spectroscopy and data analysis: Stopped-flow spectroscopy was performed at Tufts University by using a Hi-Tech Scientific SF-43 cryogenic double-mixing stopped-flow system operating in single-mixing mode. Low temperatures were maintained through the use of a liquid-nitrogen-cooled heptane bath equipped with a cryostat. To maintain an anaerobic environment, all solutions were prepared in an inert atmosphere box and transferred into the stopped-flow by using gastight syringes. Hi-Tech Scientific IS-2 Rapid Kinetics[44] software package was used to control the instrument and collect data. To ensure adequate time resolution for all processes, all reactions were monitored at time lengths ranging from 200 ms to 350 s, as appropriate. In each diode-array data set, 92 scans were acquired in a linear time base, and wavelengths were calibrated with a holmium oxide filter. For resolution of exceedingly fast processes, it became necessary to operate the system in single-wavelength mode, which yielded data with an improved signal-to-noise ratio. For each single-wavelength data set, 512 samples were collected in a linear time base.

In a typical experiment, separate solutions of **1** and a 100-fold excess of MPPH (or 100-fold excess of MPPH and 110-fold excess of proton sponge, where applicable) in 70:30 (v/v) mixture of dichloromethane and dimethylformamide were prepared and transferred into syringes in an inert atmosphere box. The solutions were then loaded into the stopped-flow instrument by syringe for use in the experiment.

Fits of kinetic data to appropriate models were performed by using the non-linear least-squares fitting methods contained in Specfit/32 version 3.0.36.[45]

Eyring analysis of the long-range (−85 to −40 °C) MPPH stopped-flow experiment (Figure S6 in the Supporting Information) was performed with the weighted linear regression package available in SPSS[46] by using a relative weighting scheme of $1/k_{obs}$ to reflect the uncertainty in the fits of the data for more rapid processes (i.e., resolution of k_1 and k_2 at higher temperatures became exceedingly difficult).

Acknowledgements

Financial support provided in part by the National Science Foundation (NSF 8238, JPC), the US Department of Energy, Office of Basic Energy Sciences (ER 14279, JPC), and the Department of Energy (DE-FG02-06ER15799, ERA). We thank the FMC Corporation for their generous donation of 70% H_2O_2.

[1] P. R. Ortiz de Montellano, *Cytochrome P-450 : Structure, Mechanism, and Biochemistry*, Plenum, New York, **1986**.
[2] B. J. Wallar, J. D. Lipscomb, *Chem. Rev.* **1996**, *96*, 2625–2657.
[3] T. J. Kappock, J. P. Caradonna, *Chem. Rev.* **1996**, *96*, 2659–2756.
[4] T. L. Foster, J. P. Caradonna, *J. Am. Chem. Soc.* **2003**, *125*, 3678–3679.

[5] W. Nam, H. J. Choi, H. J. Han, S. H. Cho, H. J. Lee, S.-Y. Han, *Chem. Commun.* **1999**, 387–388.
[6] P. A. MacFaul, K. U. Ingold, D. D. M. Wayner, L. Que, Jr., *J. Am. Chem. Soc.* **1997**, *119*, 10594–10598.
[7] I. V. Korendovych, S. V. Kryatov, E. V. Rybak-Akimova, *Acc. Chem. Res.* **2007**, *40*, 510–521.
[8] M. P. Jensen, A. M. I. Payeras, A. T. Fiedler, M. Costas, J. Kaizer, A. Stubna, E. Munck, L. Que, *Inorg. Chem.* **2007**, *46*, 2398–2408.
[9] J. T. Groves, M. Vanderpuy, *J. Am. Chem. Soc.* **1976**, *98*, 5290–5297.
[10] H. Sugimoto, D. T. Sawyer, *J. Am. Chem. Soc.* **1984**, *106*, 4283–4285.
[11] I. W. C. E. Arends, K. U. Ingold, D. D. M. Wayner, *J. Am. Chem. Soc.* **1995**, *117*, 4710–4711.
[12] P. Wardman, L. P. Candeias, *Radiat. Res.* **1996**, *145*, 523–531.
[13] R. D. Oldroyd, J. M. Thomas, T. Maschmeyer, P. A. MacFaul, D. W. Snelgrove, K. U. Ingold, D. D. M. Wayner, *Angew. Chem.* **1996**, *108*, 2966–2969; *Angew. Chem. Int. Ed. Engl.* **1996**, *35*, 2787–2790.
[14] G. T. Rowe, E. V. Rybak-Akimova, J. P. Caradonna, *Inorg. Chem.* **2007**, *46*, 10594–10606.
[15] P. J. Cappillino, G. T. Rowe, P. C. Tarves, C. E. Rogge, A. M. Spuches, A. Stassinopoulos, W. Lo, W. H. Armstrong, J. P. Caradonna, *Inorg. Chim. Acta* **2008**, in press.
[16] D. A. Whittington, S. J. Lippard, *J. Am. Chem. Soc.* **2001**, *123*, 827–838.
[17] B. F. Gherman, M. H. Baik, S. J. Lippard, R. A. Friesner, *J. Am. Chem. Soc.* **2004**, *126*, 2978–2990.
[18] M. Moche, J. Shanklin, A. Ghoshal, Y. Lindqvist, *J. of Biol. Chem.* **2003**, *278*, 25072–25080.
[19] C. Krebs, R. Davydov, J. Baldwin, B. M. Hoffman, J. M. Bollinger, B. H. Huynh, *J. Am. Chem. Soc.* **2000**, *122*, 5327–5336.
[20] B. D. Dunietz, M. D. Beachy, Y. Cao, D. A. Whittington, S. J. Lippard, R. A. Friesner, *J. Am. Chem. Soc.* **2000**, *122*, 2828–2839.
[21] A. Stassinopoulos, G. Schulte, G. C. Papaefthymiou, J. P. Caradonna, *J. Am. Chem. Soc.* **1991**, *113*, 8686–8697.
[22] M. da Silva, M. A. R. Matos, M. Ferrao, L. Amaral, M. S. Miranda, W. E. Acree, G. Pilcher, *J. Chem. Thermodyn.* **1999**, *31*, 1551–1559.
[23] W. E. Acree, G. Pilcher, M. da Silva, *J. Phys. Chem. Ref. Data* **2005**, *34*, 553–572.
[24] A. J. Everett, G. J. Minkoff, *Trans. Faraday Soc.* **1953**, *49*, 410–414.
[25] B. Perlmutter-Hayman, *Prog. Inorg. Chem.* **1976**, *20*, 229–297.
[26] S. Signorella, A. Rompel, K. Buldt-Karentzopoulos, B. Krebs, V. L. Pecoraro, J. P. Tuchagues, *Inorg. Chem.* **2007**, *46*, 10864–10868.
[27] S. Mukerjee, A. Stassinopoulos, J. P. Caradonna, *J. Am. Chem. Soc.* **1997**, *119*, 8097–8098.
[28] G. Xue, D. Wang, R. De Hont, A. T. Fiedler, X. Shan, E. Munck, L. Que, Jr., *Proc. Natl. Acad. Sci. U. S. A. Vol. 104*, **2007**, pp. 20713–20718.
[29] L. Bernasconi, M. J. Louwerse, E. J. Baerends, *Eur. J. Inorg. Chem.* **2007**, 3023–3033.
[30] H. Hirao, D. Kumar, L. Que, S. Shaik, *J. Am. Chem. Soc.* **2006**, *128*, 8590–8606.
[31] J. Kaizer, E. J. Klinker, N. Y. Oh, J.-U. Rohde, W. J. Song, A. Stubna, J. Kim, E. Muenck, W. Nam, L. Que, Jr., *J. Am. Chem. Soc.* **2004**, *126*, 472–473.
[32] S. K. Lee, J. C. Nesheim, J. D. Lipscomb, *J. Biol. Chem.* **1993**, *268*, 21569–21577.
[33] R. N. Austin, H. K. Chang, G. J. Zylstra, J. T. Groves, *J. Am. Chem. Soc.* **2000**, *122*, 11747–11748.
[34] A. M. Valentine, B. Wilkinson, K. E. Liu, S. KomarPanicucci, N. D. Priestley, P. G. Williams, H. Morimoto, H. G. Floss, S. J. Lippard, *J. Am. Chem. Soc.* **1997**, *119*, 1818–1827.
[35] S. Y. Lee, J. D. Lipscomb, *Biochemistry* **1999**, *38*, 4423–4432.
[36] D. Rinaldo, D. M. Philipp, S. J. Lippard, R. A. Friesner, *J. Am. Chem. Soc.* **2007**, *129*, 3135–3147.
[37] P. E. M. Siegbahn, *J. Biol. Inorg. Chem.* **2001**, *6*, 27–45.
[38] L. J. Shu, J. C. Nesheim, K. Kauffmann, E. Munck, J. D. Lipscomb, L. Que, *Science* **1997**, *275*, 515–518.
[39] K. E. Liu, A. M. Valentine, D. L. Wang, B. H. Huynh, D. E. Edmondson, A. Salifoglou, S. J. Lippard, *J. Am. Chem. Soc.* **1995**, *117*, 10174–10185.
[40] S. K. Lee, B. G. Fox, W. A. Froland, J. D. Lipscomb, E. Munck, *J. Am. Chem. Soc.* **1993**, *115*, 6450–6451.
[41] M. M. Palcic, H. B. Dunford, *J. Biol. Chem.* **1980**, *255*, 6128–6132.
[42] R. R. Hiatt, W. M. J. Strachan, *J. Org. Chem.* **1963**, *28*, 1893–1894.
[43] D. A. Skoog, D. M. West, F. J. Holler, *Fundamenals of Analytical Chemistry*, 7th ed., Harcourt Brace & Company, Orlando, **1996**.
[44] Hi-Tech Scientific, Bradford on Avon, UK, **1999**.
[45] R. A. Binstead, A. D. Zuberbühler, B. Jung, 3.0.36 Ed., Spectrum Software Associates, Chapel Hill, NC, **2004**.
[46] 15.0 ed., SPSS Inc., **2007**.

Received: February 14, 2008
Published online: August 4, 2008

